

# MONITORING OF A STEEL-LINED PRESSURE SHAFT USING GLOBAL INDICATORS AND THE FREQUENCY RESPONSE FUNCTION

Fadi E. Hachem<sup>1</sup> & Anton J. Schleiss<sup>2</sup>

<sup>1</sup>Dr. sc. and Project Manager, STUCKY SA, rue du Lac 33, 1020 Renens VD1, Switzerland

<sup>2</sup>Professor and Director, Laboratory of Hydraulic Constructions (LCH-EPFL), Ecole Polytechnique Fédérale de Lausanne, Station 18, 1015 Lausanne, Switzerland

E-mail: fhachem@stucky.ch, anton.schleiss@epfl.ch

## Abstract

Due to high peak energy demands, existing hydropower plants operate nowadays under rough conditions to regulate the discharge and power with relatively fast and repeated opening and closing of turbines and pumps.

The local deterioration of the mechanical properties of the steel-lined pressure wall induces a change of the two global indicators: the water-hammer celerity and the wave attenuation. This deterioration may arise from the weakening of the backfill concrete and/or the surrounding rock mass.

In-situ measurements of the pressure shaft of the Grimsel II pumped-storage plant in Switzerland have been carried out to monitor these global indicators and to determine its frequency response function. The prototype measurements use dynamic pressure sensors placed at both ends of the pressure shaft. The data are acquired continuously and accessed on-line via internet. Different approaches to estimate the wave speed and wave attenuation coefficient generated inside the pressure shaft during start-up and shut-down of pumps and turbines have been applied. The wave speed was assessed from the Fourier transformation spectrums while the attenuation coefficient was determined by computing the root mean square of the signal followed by an exponential regression fitting. Monitoring charts have been established based on the statistical quality control method. The control limits and the overall behavior of the pattern of future measured points will be used for on-line monitoring of the shaft. The magnitudes of the frequency response function of the system and the coherence of pressure signals have been also defined. In spite of many difficulties encountered during the in-situ measurements, the results show a stable monitoring scheme of the wave speed and wave attenuation coefficient. Longer acquisition data series are needed to consolidate the control limits. The response identification function of the pressure shaft was not very efficient in this special case because of the reflection of the major part of the wave by the junction located between the pressure and surge shafts of the plant.

## Introduction and Motivation

In former years, the safety margin for water-hammer load in steel-lined pressure tunnels and shafts of hydropower plants was considered as acceptable. Nowadays, the high energy demands force the existing plants to operate under severe conditions with relatively fast valve opening or closing to regulate the discharge. This generates higher water-hammer loads which may lead to a local deterioration of the backfill concrete and the near rock field surrounding the liner. Thus, the load distribution ratio between the three components steel, concrete and rock of the wall system will be modified and the stresses in the steel liner may generate yielding in the case of traditional steel or crack initiation and propagation for high-strength steel. In the worst case, brittle failure of the steel liner can occur and may produce catastrophic landslides due to hydraulic jacking of the surrounding rock mass. Therefore, non-intrusive monitoring and control methods for existing steel-lined pressurized shafts and tunnels need to be enhanced.

A drop of radial stiffness of steel-lined shafts and tunnels induces a drop of wave speed values and an increase of the wave attenuation due to the transmission/reflection phenomenon (Wylie, Suo, & Streeter, 1993) and (Hachem & Schleiss, 2012). A transient based assessment method for detecting the formation of weak reaches by monitoring the celerity and the attenuation of the wave inside the pressure shaft of a pumped-storage power plant is presented in this paper. These indicators are estimated from the pressure data acquired during the water-hammer phenomena generated by normal closing and opening of pumps and turbines at the powerhouse.

## In Situ Measurements

### Description of the site

The Grimsel II pumped-storage power plant is located in the Canton of Bern, in the central part of Switzerland. The plant, owned by Kraftwerke Oberhasli AG (KWO), has an underground powerhouse, equipped with four separated pump-turbine units with a total installed capacity of

350 MW. A 4 km long headrace tunnel with an internal diameter of 6.8 m connects the Lake Oberaar (the upper reservoir) to the vertical 123 m high surge tank of 13 m in diameter. A security butterfly valve is installed downstream of the surge tank and followed by the steel-lined shaft which has an internal diameter of 3.8 m and a length of about 750 m. The upstream end of the shaft is connected to a 170 m long inclined tunnel of 4.14 m of internal diameter. It is the extension of the pressure shaft excavation (Figure 1) and functions together with the main surge tank as an inclined surge shaft. The steel-lined pressure shaft has a slope of 100 % (45°) and conveys water from the upper reservoir to the powerhouse. An accessible steel-liner reach of about 1.5 m is located just upstream of the bifurcation which distributes the water at the high pressure side to the four machines inside the powerhouse.

Figure 1 shows a schematic view of this water conveyance system, including the shaft, the surge tanks and the powerhouse. The locations of the measurement stations S1 and S2 and the lateral cross-section of the steel-lined shaft are also shown.

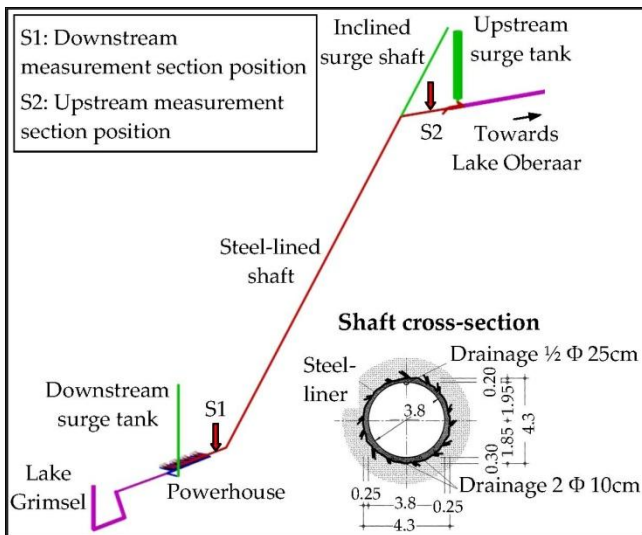


Figure 1: Schematic view of the waterway system of the Grimsel II pumped-storage plant with the two positions of the data acquisition systems and a cross-section of the steel-lined shaft.

### Measurement instrumentation and data acquisition

Two dynamic piezoresistive pressure sensors of type “Kistler 4045A” with an absolute pressure range of 100 bars (for the measurement station S1) and 20 bars (for station S2) have been used. The sensitivities of these sensors are equal to 5 mV/bar and 25 mV/bar for the former and latter, respectively. The constant DC electrical excitation current of 24 V needed for these sensors, is provided after transformation of the 48 VDC current available in the powerhouse and in the security valve cavern. These pressure sensors are calibrated by the

manufacturer and the output signals are amplified by a “Kistler 4618A2” amplifier type.

At the measurement station S1, the pressure sensor is screwed inside a hole made in the elbow of the shaft drainage conduit of 150 mm in diameter (Figure 2a). At the measurement station S2 shown in Figure 2b, the pressure sensor is fixed on the cover plate of the shaft drainage reach of 200 mm in diameter.

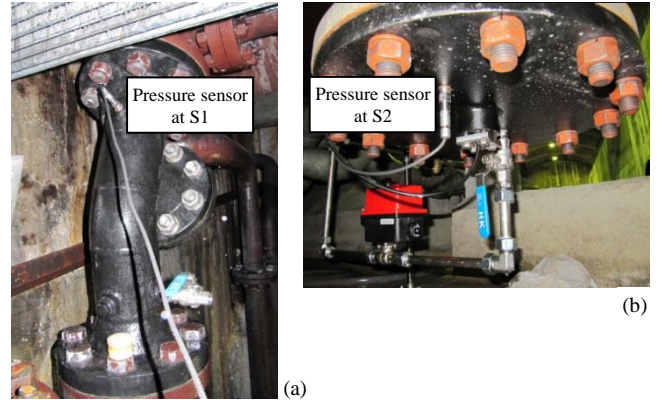


Figure 2: Pressure sensors at the measurement stations of the steel-lined pressure shaft of the Grimsel II plant, (a) at station S1 and (b) at station S2.

Each of the two data acquisition systems at S1 and S2 contains also one “NI-USB-6259 M series” acquisition card and one industrial PC (Figure 3). The total output current of the existing Venturi flow measurement system has been transformed to voltage (through a box of electric resistances) and then inserted inside the acquisition card at S1. The control command of the valves in the powerhouse, sent from the control center, is transformed by an electric relay to a trigger signal of 0-10-0 VDC with a plateau of 3 s. The trigger output signal has been connected to the measurement system at S1.

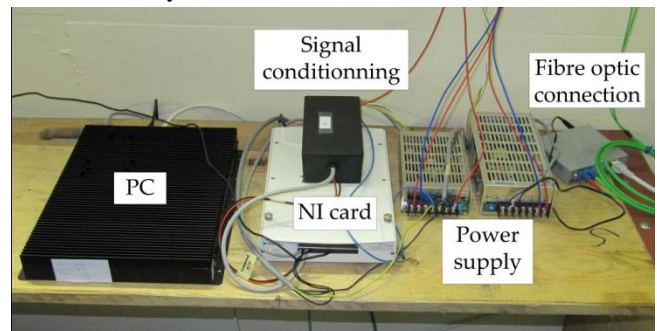


Figure 3: Installed acquisition system at the measurement stations in the Grimsel II pumped-storage plant.

The synchronization of the two acquisition systems at S1 and S2 is done via a fiber optic cable which connects the two system PCs to the KWO server inside the powerhouse. Every one hour, the internal clocks of the two PCs are automatically synchronized with the KWO server time. The trigger signal acquired at S1 is saved by the acquisition software as a shared variable type (LabVIEW, 2008) and sent to the PC of station S2. This type of network-published

variables can be used to write and read across an Ethernet network. The two measurement systems can be controlled via a VPN internet connection (Virtual Private Networking). The acquired data can be accessed on-line through a secure VPN internet connection.

The data acquisition software is based on LabVIEW programming platform. The data are acquired continuously in time at a sample frequency of 1 kHz and they are not stored until the trigger signal rises from 0 to 10 V. The total storage time has been fixed to 600 s and includes the steady-state and the transient parts of the pressure and vibration signals. In each PC of the two measurement systems, the storage loop starts by opening a data file of format TDMS and assigning the date given by the PC clock to the storage directory name. This loop ends automatically after the collapse of the storage duration fixed by the user.

## Analysis of Prototype Results

### Output data

The transient data acquired from the in-situ monitoring system are generated by service loads induced by the normal start-up and shut-down of the pumps and turbines. An example of these data generated by the shut-down of turbines is given in Figure 4a and 4b. These signals are acquired after the complete closure of the control valves of turbines. The drop of the mean pressures is caused by the mass oscillation phenomenon of low frequency.

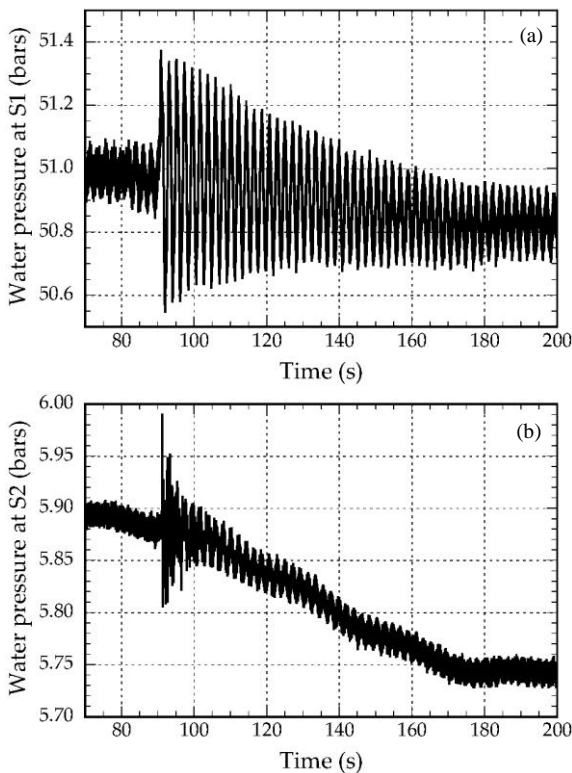


Figure 4: Example of pressure records used for monitoring of the pressure shaft after the shut-down of turbines, (a) at station S1 and (b) at station S2.

### Estimation of the water-hammer wave speed

A first estimation of the water-hammer wave speed inside the pressure shaft is obtained by the Fast Fourier Transform (FFT) applied to the pressure records at S1. The FFT with Hanning windowing has been used and the normalized RMS FFT density spectrums of the 396 acquired files during pumping and generating modes have been computed. For each of these modes, the corresponding FFT of all the pressures at S1 show the same pattern as in Figure 5. The FFT spectrum shows clearly a strong peak near frequency 0.46 Hz with weaker peaks at higher frequencies. The 0.46 Hz is the fundamental frequency,  $f_{fund}$ , of the shaft. It corresponds to the water-hammer propagation between the downstream end of the distributor and the main reflection border located at the junction between the pressure and the surge shafts. Thus, the wave speed  $a$  can be estimated from the following formula:

$$a = 4 \cdot L \cdot f_{fund} \quad (1)$$

where,  $L$  is the shaft length between the end of the distributor inside the powerhouse and the intersection of the pressure shaft with the inclined shaft. For  $L$  equal to 762.3 m, the estimated wave speed is  $1402.7 \pm 23.5$  m/s for a minimum FFT resolution of  $\pm 0.0077$  Hz. The wave speed values estimated by the FFT approach for all the 396 files acquired between February 17 and June 10, 2011 have a mean and standard deviation 1433.3 m/s and 35.7 m/s, respectively.

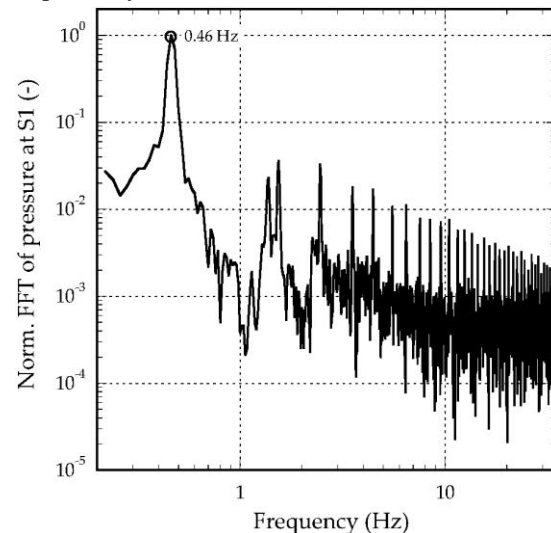


Figure 5: Example of the normalized FFT spectrum of pressures acquired at S1 during shut-down of turbines.

The second estimation approach of the wave speed is done by using the two pressure sensors at S1 and S2. Different time-based techniques have been used to estimate the travel time between the pressure sensors and the results of the most adequate techniques for each pumping and generating

modes have been adopted (Hachem, 2011). The pressure records were filtered by using Daubechies (db10) mother wavelet (Mallat, 1990) before the estimation of the travel time. For each record, the summation of the decomposition details from D8 to D12 has been considered. The wave speed values estimated from the time lag between the pressures at S1 and S2 show scattered patterns relative to the values obtained from the FFT approach. The former approach is probably affected by the following important sources of error: (i) the unknown synchronization time delay of the internal clocks of the PCs of the two acquisition systems, (ii) the alteration and dispersion of the pressure signals, and (iii) the accuracy of the assessment methods. Regarding the first point, the synchronization of the pressure transducers was an issue because of the important distance between the measurement sections of the pressure shaft. In spite of the fact that important effort has been invested to build the synchronization scheme, the results show that the method adopted was not reliable. In fact, the server used to synchronize the internal clock of the PCs is located inside the powerhouse. Therefore, the time needed by the two acquisition systems to access the server is not exactly the same. For example, an accuracy in the order of 100 ms induces an error of around 20 % on the wave speed between sensors. Another method of synchronization which does not use the internal clock of the PCs, consists in sending an electrical current pulse at the moment of trigger from the powerhouse towards the upstream measurement station. This method is more accurate than the one that has been used. Unfortunately, its application to the Grimsel II plant was not possible because of the absence of an electrical cable connecting the two measurement stations. The second source of error is related to the alteration, dissipation and dispersion of the water-hammer wave when it crosses the junction between the headrace pressure tunnel and the inclined surge shaft. At this junction, the major part of the wave energy (above 75 %) is reflected back to the powerhouse. The special waterway layout of the Grimsel II plant with an inclined surge shaft located between the two measurement stations has significantly reduced the efficiency of the applied methods used to estimate the wave speed values. Finally, the accuracy of the assessment methods is closely related to noise level which affects the measurement records. The mean signal to noise ratio at station S1 was around 1241. The reflection of the water-hammer wave at the surge shaft junction has reduced this ratio to 169 for the measurements at station S2. The decrease of the signal to noise ratio induces higher error in the computed travel time of the wave between the pressure sensors and reduces the accuracy of the determination of the wave speed. It may be concluded that the estimation of the wave speed according to the FFT approach applied to the pressure

records at station S1 of the Grimsel II plant is more accurate than the methods based on processing the two pressure sensors at S1 and S2. Therefore, the FFT approach was used to establish the monitoring charts for the water-hammer wave speed.

### Estimation of the wave dissipation coefficient

The wave dissipation has been quantified by using the exponential dissipation coefficient obtained from the pressure  $p_1$  at S1.

The dissipation coefficient,  $b_2$ , is defined as the exponential coefficient of the following equation (Hachem & Schleiss, 2011):

$$\frac{\text{RMS}(p_1)}{\max[\text{RMS}(p_1)]} = b_1 \cdot e^{b_2(t/T_{\text{fund}})} \quad (2)$$

where,  $\text{RMS}(p_1)$  and  $\max[\text{RMS}(p_1)]$  are the Root Mean Square of the pressure  $p_1$  and its maximum value, respectively,  $(t/T_{\text{fund}})$  is a dimensionless variable in which  $t$  is the time and  $T_{\text{fund}}$  is the fundamental period of the pressure shaft, and  $b_1$  is the normalized RMS value at  $t=0$ . The parameters  $b_1$  and  $b_2$  of equation (2) have been estimated by fitting an exponential regression curve on the normalized RMS values of the filtered pressure signal  $p_1$ . The pressure records are filtered by using Daubechies (db10) mother wavelet where only details from D8 to D12 have been retained. The resolution of the RMS is taken equal to  $1000 \text{ Hz} / 0.46 \text{ Hz} \approx 2175$ . The results reveal the existence of two different families of  $b_2$  with a mean of -0.078 and a standard deviation of 0.015 for the pump and turbine start-up modes and a mean and standard deviation of -0.035 and 0.015, respectively, for the shut-down modes. The relative difference between the  $b_2$  means is about 55 %. The higher wave dissipation detected in the pump and turbine start-up modes can be explained by the fact that additional wave dissipation is encountered by the opened bypass of the spherical valve inside the powerhouse. This boundary condition of the pressure shaft can also explain the scattering of the dissipation coefficient values in this mode.

### Frequency response function of the pressure shaft

The system identification is an approach used to characterize a physical system in a quantified way (Shin & Hammond, 2008). The ultimate objective of this approach is to estimate the frequency response function  $H(f)$  of the system considered as linear and time invariant (LTI) with stationary random input signal.

The system identification approach was used to assess the pressure measurements at S1 and S2 of the pressure shaft of the Grimsel II power plant. Figure 6 shows the frequency response functions  $H(f)$  for the pumping and generating

modes. Each response curve is obtained by averaging five measurement data histories acquired in February between 13 and 29, 2011. Unlike the good identification results obtained from the experimental data generated inside a test pipe of a physical set-up (Hachem, 2011), the magnitude of the response functions do not show peaks at the fundamental frequency (0.46 Hz) of the pressure shaft. The failure of this method is due probably to the reflection of the major part of the wave by the junction located between the pressure and surge shafts. Nevertheless, the coherence function given in Figure 7 shows interesting linearity of the system (coherence is close to 1) near frequencies 0.46 Hz, 1.38 Hz, and 2.30 Hz. The two latter frequencies are the third and fifth harmonics which have been also detected by the FFT approach presented in Figure 5.

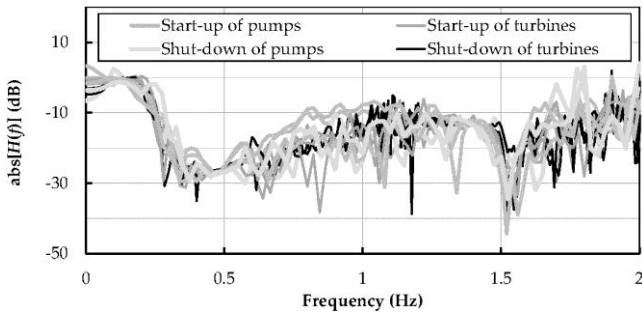


Figure 6: Magnitude spectrum of the frequency response function  $H(f)$  obtained from the pressure data at stations S1 and S2 of the pressure shaft of the Grimsel II power plant.

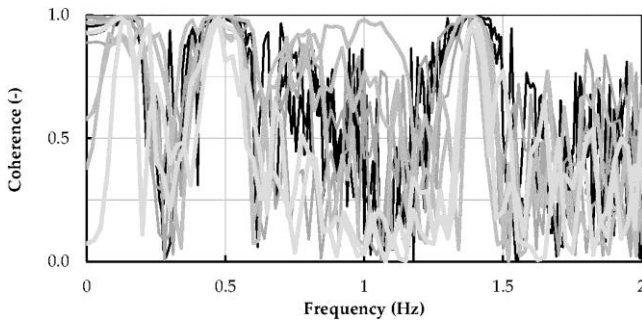


Figure 7: Coherence function of the pressure data at stations S1 and S2 of the pressure shaft of the Grimsel II power plant.

### Monitoring charts

The development of monitoring charts for the wave speed and the exponential dissipation coefficient have been inspired from procedures used in statistical quality control (Montgomery, 2005). The control or monitoring chart is a graphical display of the feature that has been measured or computed from a data sample versus the sample number or time. It contains a center line (CL) that represents the average value of the feature corresponding to the in-control state and two other horizontal lines, called the upper control limit (UCL) and the lower control limit (LCL). These control limits are chosen in a way that the process will be

considered in control if nearly all the sample points fall between them. For variables such as the wave speed and the dissipation coefficient, both the mean of the estimated values and their variability are used. The control of the process average or mean quality level is done with the so-called  $\bar{x}$  chart while the process variability is monitored with a control chart for the range, called  $R$  chart. The former monitors between-sample variability (variability in the process over time) while the latter measures within-sample variability (the process variability between each sample at a given time).

Figure 8a shows an example of the  $\bar{x}$  monitoring chart of the wave speed inside the pressure shaft of the Grimsel II plant. The  $R$  chart is presented in Figure 8b. The control limits have been defined by classifying 396 subsequent records in 66 subgroups of 6 samples each (the filled squares in Figures 8a and 8b). The statistical quality control method considers that the variable  $x$  is normally distributed. Yourstone and Zimmer (1992) shows that samples of size  $n > 4$  are sufficient to ensure normality assumption. For  $n = 6$ , the mean and the standard deviation of the relative range variable are 2.534 and 0.848, respectively (Montgomery, 2005).

All the points fall inside or near the control limits of  $\bar{x}$  chart and no systematic pattern behavior is detected. Also, the points plotted on the  $R$  chart do not show a specific pattern behavior but they have four points, between April 27 and May 22, that fall relatively far above the UCL limit. These points are generated by the unusually high values of the wave speed during the same period of time. All these high values are computed from pressures acquired during the pumps and turbines start-up modes. It is clear that the control limits of the monitoring charts can be revised by discarding the points that are out-of-control and by using only the remaining in-process points. Such adjustment will be more relevant if it is done after acquiring a longer series of in-situ measurements. Dealing with the available data, the observations indicate that the process is in control in the present time and the control limits defined are suitable and reliable for controlling current and future wave speed values. The general patterns of points on the  $\bar{x}$  and  $R$  charts reveal that the data assessment method proposed in this section for estimating the wave speed is stable since no change of the stiffness of the steel-lined shaft is suspected to happen in the short time duration of this monitoring. Any decrease of future wave speed values induced by a drop of the wall stiffness of the pressure shaft should be detected on the  $\bar{x}$  chart by a permanent decrease of mean values with more or less the same global behavior of  $R$ . The failure of the acquisition system and/or the assessment methods should appear on the  $R$  chart by a high scattered pattern of points falling far outside the established control limits.

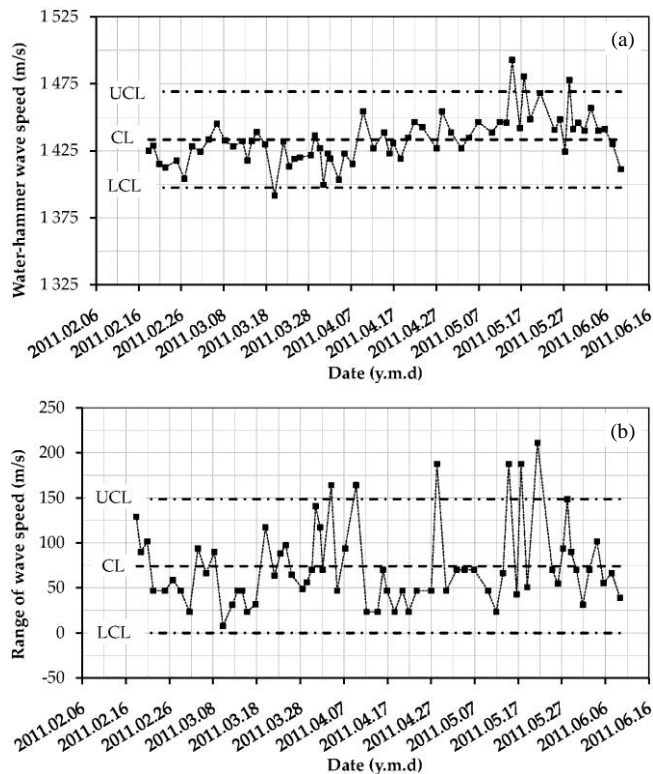


Figure 8: The transient based monitoring charts for the wave speed of the pressure shaft of the Grimsel II pumped-storage power plant, (a)  $\bar{x}$  chart and (b)  $R$  chart.

### Conclusion

The water-hammer pressures inside the steel-lined pressure shaft of the Grimsel II pumped-storage plant in Switzerland have been measured with two high sensitive sensors located at the entrance of the powerhouse (station S1) and at the security butterfly valve (station S2). The transient signals generated by the maneuvers of the valves and machines during pumping and generating modes have been recorded during four months between February 17 and June 10, 2011. A total number of 396 data files have been acquired continuously in time at a sample frequency of 1 kHz and they have been controlled and accessed on-line by a secured VPN internet connection. The signals were analyzed to assess the water-hammer wave speed and to quantify the wave attenuation inside the steel-lined pressure shaft. The special layout of the latter with its inclined surge shaft situated between the upstream and downstream measurement stations and the low accuracy of the synchronization scheme between the two acquisition systems made it difficult to use the two pressure records at stations S1 and S2 to estimate the celerity and attenuation of the water-hammer wave. Nevertheless, it was possible to monitor the shaft by processing data only at station S1. The wave speed was assessed from the FFT density spectrums while the attenuation coefficient was determined by computing the RMS of the filtered pressure signal followed by an exponential regression fitting. The monitoring charts

of the mean  $\bar{x}$  and the range  $R$  were established based on the statistical quality control procedure.

The general patterns of points on the  $\bar{x}$  and  $R$  charts reveal that the data assessment method for estimating the wave speed and attenuation is stable. Any decrease of future wave speed values and/or increase of wave attenuation coefficient induced by a drop of the wall stiffness of the pressure shaft should be detected on the monitoring charts by a permanent deviation of mean  $\bar{x}$  values with more or less the same global behavior of  $R$ . The failure of the acquisition system and/or the assessment methods should appear on the  $R$  chart by a high scattered pattern of points falling far outside the established control limits. The control limits for the water-hammer wave speed can be updated after acquiring a longer series of in-situ measurements.

The proposed monitoring procedure is based on a continuous acquisition of the transient pressure signals and calculating the wave speed and attenuation. Once a significant and persistent change of these parameters is detected, a drop of the wall stiffness is suspected to be occurred somewhere along the shaft. The pressure FFTs and the frequency response function  $H(f)$  should reveal also new peaks at frequencies that corresponds to reflections from the weak reaches.

### References

Hachem, F. (2011). Monitoring of steel-lined pressure shafts considering water-hammer wave speed and fluid-structure interaction. Switzerland: PhD thesis No 5171, Ecole Polytechnique Fédérale de Lausanne.

Hachem, F., & Schleiss, A. (2012). Effect of Drop in Pipe Wall Stiffness on Water-Hammer Speed and Attenuation. *Journal of Hydraulic Research*, Accepted for publication.

Hachem, F., & Schleiss, A. (2011). On-line monitoring of steel-lined pressure shafts and tunnels by using pressure transients under normal operation conditions. *Journal of Hydraulic Engineering*, Submitted for publication.

LabVIEW. (2008). National Instruments. Release 8.6. [www.ni.com/labview/](http://www.ni.com/labview/).

Mallat, S. (1990). A wavelet tour of signal processing. San Diego, CA: Academic Press.

Montgomery, D. (2005). Introduction to statistical quality control. USA: John Wiley and Sons, fifth edition.

Shin, K., & Hammond, J. (2008). Fundamentals of signal processing for sound and vibration engineers. New York: John Wiley and Sons.

Wylie, E., Suo, L., & Streeter, V. (1993). Fluid Transients in Systems. Prentice Hall, Englewood Cliffs, NJ: facsimile edition.

Yourstone, S. & Zimmer, W. (1992). Non-normality and the design of control charts for averages. *Decision Sciences*, 23(5):1099–1113.